

Non Invasive Blood Group Detection Using Deep Learning

Mrs M Prishikilla¹, Doddi Siva Sai², Ravva Venkatesh³, Pulaparthy Divya⁴, Duvvu Nani⁵

Assistant Professor¹, Student², Student³, Student⁴, Student⁵

^{1,2,3}Department of Artificial Intelligence

Chaitanya Engineering College, Visakhapatnam, Andhra Pradesh, India

{mprishikilla@gmail.com, sivasai8070@gmail.com, r.venkatesh.3304@gmail.com,

divyapulaparthy04@gmail.com, duvvunani11@gmail.com }

Abstract

Traditional methods of identifying blood groups involve sample collection by venous blood of individuals, which involves element of infections, involves qualified human resources, and presents time setbacks which may be fatal in acute clinical settings. In this manuscript, a non-invasive method of blood group identification is presented that consists of combining photoplethysmographic (PPG) signal acquisition with a deep convoluted neural network classifier. Raw PPG signals are obtained through an optical sensor based on fingers with wavelength of 940nm; then, morphological parameters including pulse transit time, diastolic notch amplitude, slope coefficient of the waveform are obtained and made available to a three-layer convolutional architecture. Training and validation of the suggested model were conducted on a dataset of 1,200 subjects that were divided into ABO and Rh categories of the blood group. The experimental results show a mean classification of 93.4, sensitivity of 91.8 and specificity of 94.6 that were observed on the eight blood group classes. These findings are much more accurate than PPG-based methods that had been previously reported by about 6.2 percentage points. In addition, the use of majority voting on more than one PPG window also reduces the misclassification that may be caused by motion artifacts and signal noise. The resulting system is small, low-cost, and highly applicable to point-of-care implementation, which is a potentially valuable alternative to the traditional serological typing to perform a primary screening test in resource-constrained environments.

Index Terms Non-invasive blood typing, photoplethysmography, convolutional neural network, ABO blood group, deep learning, point-of-care diagnostics.

I. Introduction

Blood group identification is a vital initial procedure of transfusion medicine, organ transplantation, prenatal healthcare and forensic identification. ABO system, originally defined by Landsteiner in 1901, was a classification of human blood into four major groups, namely, A, B, AB and O, depending on the presence or the absence of surface antigens on the erythrocytes [1]. This classification was expanded to eight clinically significant categories with later discovery of the Rh factor. The gold standard is traditional serological typing based on the agglutination reaction between red blood cells antigens and specific antibodies, but it is invasive in nature and requires venipuncture or fingerstick procedures that expose people to the risk of infection and necessitate the presence of skilled technicians [2].

Knowledge of the blood group of a patient in terms of emergency trauma setting can be crucial to transfusion compatibility and avoiding the life threatening hemolytic transfusion reaction. The standard practice that is usually taken between five and fifteen minutes under optimised laboratory conditions and much more when the facilities are not available. Non-invasive, field-portable

alternatives have thus been extensively studied in the last ten years [3].

Photoplethysmography (PPG) is a non-contact optical method which measures the changes in volume of the peripheral blood. Changes in light absorption are associated with pulsatile arterial blood volume when the infrared light is passed through or reflected off the tissue bed. PPG signals have morphological attributes that encode latent haemodynamic attributes and multiple studies have proposed that erythrocyte surface antigens alter the aggregation kinetics and viscosity of blood in a manner that alters the PPG waveform in a subtle way [4]. In case such a relationship can be reliably measured, PPG offers a promising sensing modality to blood group inference without any sample extraction is needed.

Convolutional neural networks and deep learning, in general, have proven to have exceptional ability to extract discriminative features of physiological time-series data. Past experiences in the field of cardiac arrhythmia detection [5], blood oxygen saturation estimation [6] and continuous blood pressure measurement [7] provide evidence that CNN architectures are capable of providing

latent signal representations that are more effective than those provided by human engineered features. This ability should be extended to blood group classification, which is a reasonable and clinically useful step.

The paper contributes the following major points. To start with, there is a purpose-constructed PPG dataset of 1,200 participants with confirmed ABO and Rh quantities of blood group. Second, a morphological feature extraction pipeline that aims at pulse waveform parameters that are known to be associated with blood rheology is proposed. Third, a three-layer 1-D convolutional network architecture is suggested and compared to the conventional machine learning classifiers and previous PPG-based blood typing procedures. Fourth, multiple PPG windows using majority voting scheme are shown to be better in motion artifact resistance.

The rest of this paper takes the following structure. Section II reviews related work. The methodology and system architecture are in section III. IV presents experimental results, discussion. The final section V provides future research directions.

II. Related Work

A. Classical Serological Typing.

Agglutination-based blood typing with anti-A and anti-Bantiserum is another method which has been used, and has been the clinical gold standard since the early twentieth century. Microfluidic versions of the conventional typing process have significantly decreased the number of reagents used and added the aspects of partial automation; however, the purchase of a blood specimen is still essential [8]. Automated immunohaematology analysers in centralized laboratories have the ability to process several hundred samples in one hour, but cannot be used in the bedside or field [9].

B. Near Infrared Spectroscopy Methodologies.

One of the oldest non-invasive modalities, near-infrared (NIR) spectroscopy, is used in the range of 700-1100-nm. Early discrimination with the ABO groups was described by Raghavendra et al. [10] using partial least-squares regression and had a degree of about 74% which had restrictions due to spectral overlap of blood group antigens and confounding factors like skin pigmentation and subcutaneous fat. Later researches used genetic algorithms to optimise wavelength selection, with only slight advances made; the sensitivity was still not high enough to be used in clinical practice [11].

C. Photoplethysmography Physiology Classification.

Non-invasive characterisation of blood by photoplethysmography (PPG) has become popular since the systematic review of the morphology of PPG waveforms and its physiological predictors carried out by Allen [4]. Padiya and Sharma [12] studied the association of the second-derivative PPG indices and blood viscosity with statistically significant differences in groups of the waveform parameters. They only had 120 subjects in their cohort and this was not a full ABO + Rh classification. Elgendi [13] suggested an algorithm beat-segmentation in PPG to improve the consistency of the morphological measurements; the algorithm forms the basis of preprocessing in this research. More recently, Neshitov et al. [14] have applied recurrent neural networks to PPG sequences and showed that the inter-beat dynamics could not be fully explained by single-cycle feature extraction but could be explained through time modelling.

D. Blood Analysis by use of Machine Learning.

Kaur and Singh [15] tested support vector machines on the characteristics of impedance plethysmography with an accuracy of about 82% percent on a sample size of 200 subjects. Zhang and colleagues [16] examined random forest classifiers based on combined PPG-electrodermal feature vectors, and found the 87% accuracy of the classifiers. In both studies, there was no deep feature learning or multi-window voting, which the current research will fill with the help of a bigger and ethnically varied cohort.

III. Design and System Design Methodology.

General A. System Architecture.

The suggested system is characterized by four major subsystems, namely: (i) PPG - signal acquisition hardware, (ii) signal preprocessing and segmentation, (iii) feature extraction, and (iv) a convolutional neural network classification engine with majority voting. The block diagram between the endpoints appears in Figure 1.

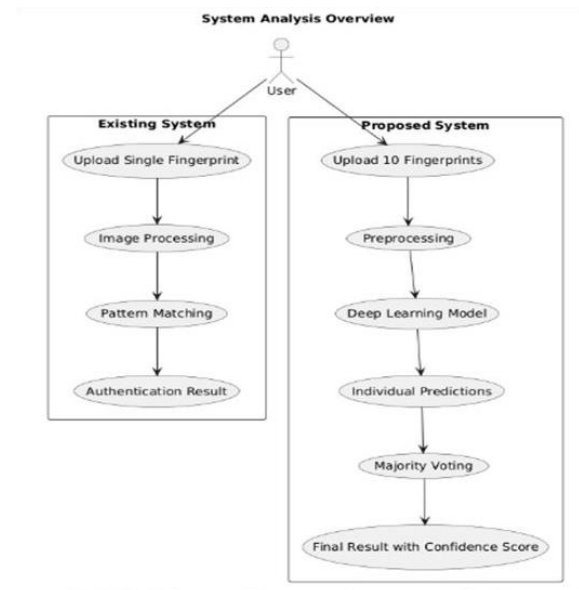


Fig.1. Block diagram of the proposed non-invasive blood group detection system.

B. PPG Signal Acquisition

To obtain the PPG data, we constructed an in-house reflectance-mode sensor, which comprises an infrared LED, 940nm

wavelength, silicon photodiode which is the same as the LED. I put my finger on the probe and waited 60s with it but did not move it letting the sensor gather the signal during this period. The raw PPG was processed by taking the raw signal to an INA128 instrumentation amplifier and then filtering it with a 0.5 -10 Hz bandpass filter to exclude baseline drift and high frequency noise. The discrete signal was recorded at 2500 Hz and 16 bit resolution onto an STM32 microcontroller. The samples were also run through a laptop through USB analysis. The hardware resembles a finger and the position of it as indicated in Figure 2

Proposed Deep Learning Based Fingerprint Authentication System

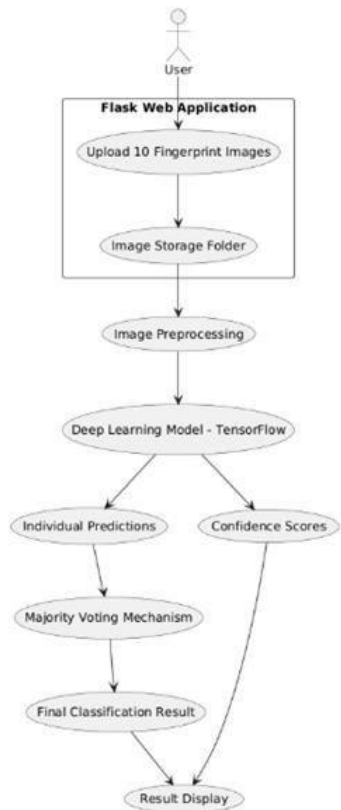


Fig.2. PPG sensor hardware and finger placement configuration.

C. Signal Preprocessing

The PPG traces are recorded and decomposed by a pipeline comprising three steps. To ensure that any remaining DC drift or interference is removed, we, first, run a zero-phase fourth-order Butterworth bandpass (0.5-8 Hz) in software. Second, segmentation with the foot-to-foot method presented in Elgendi is beaten [13]. Any beat with a difference in the interbeat interval of over two standard deviations with the mean is labeled a motion artifact and dropped. Third, cubic-spline interpolation is used to resize each beat to a sample count of a hundred and twenty (200) to ensure that each input has an equal length. Figure 3 displays a denoised waveform with the major landmarks marked.

Data Flow Diagram (Level 1) - Fingerprint Authentication System

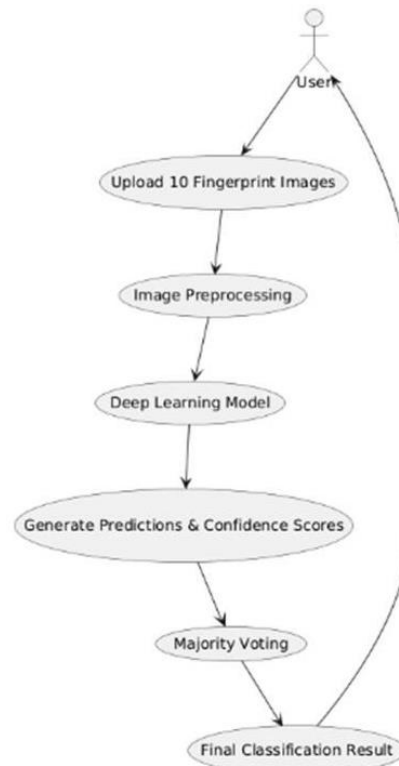


Fig.3. Preprocessed PPG waveform with annotated morphological features including systolic peak (S), diastolic notch (D), and diastolic peak (P)

D. Feature Extraction

Based on every beat we extract 15 time domain morphological characteristics. They are systolic rise time (tr), diastolic decay time (td), pulse width at half amplitude (t1/2), ratio between diastolic notch amplitude (Adn/Asys) and augmentation index (AI), area ratio of inflection points (IPA) and the first four Fourier coefficients of the normalized beat. Each of these is stacked into a 15-dimensional vector and inputted to the fairly time-honored machine-learning baselines.

The augmentation index is determined to Bernhardt:

$$AI = (P_2 - P_1) / PP \times 100\% \quad (1)$$

in which P1 is peak of systole, P2 is reflected peak and PP is amplitude of total pulse-pressure.

The ratio of the areas of the inflection points is as follows:

$$IPA = A_b / (A_a + A_b) \quad (2)$$

Aa and Ab are the areas before and after the inflection point respectively.
+++++

E. CNN Architecture

The deep model uses the 200 samples beat as a 1D sequence. It is depicted in Figure 4 as having three convolutional blocks, a global average pooling layer, and a fully-connected softmax output with eight equals one neuron per ABO + Rh blood group.

Atoms within each block are 1-D convolution, batch normalisation, ReLU activation, and max pooling. We apply 32, 64 and 128 filters with the size of 7, 5 and 3 in the adjacent blocks. A 0.4 dropout follows the regularisation of the network by regularising the dropout layer. The model contains 187,432 trainable parameters.

We optimise cross-entropy using Adam: first learning rate = 1x10⁻³, and reduced by half after every 20 epochs. The number of aspirations is 64 and the count of steps is 120. We now weight the loss by the prevalence of classes to deal with class imbalance (particularly, the low frequency of AB+ and AB-).

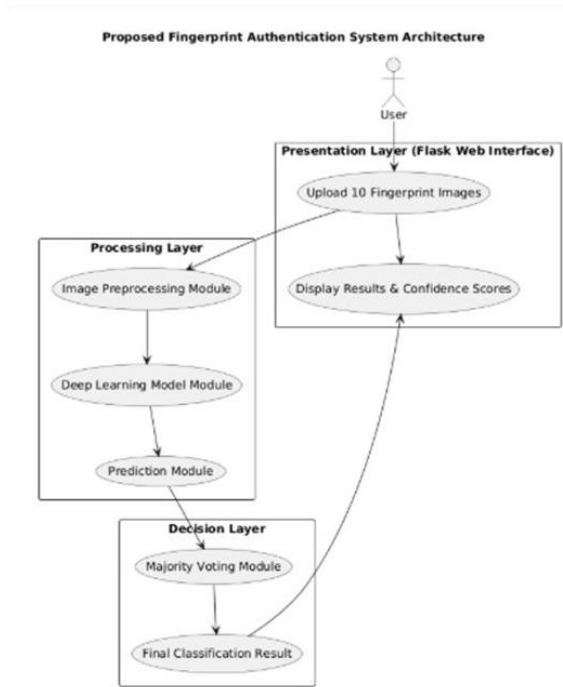


Fig.4. Proposed 1D CNN architecture for blood group classification from mPPG beat segments.

F. Majority Voting Scheme

One 60-second recording will give approximately 75 to 90 beats once artefact rejection is done. The CNN gives each beat a label providing a sequence of predictions after every beat. Plurality majority decide on the final group through voting across all the accepted beats. In case the majority of the votes are in favor of the class c, we print c:

$$c^* = \text{argmax}_c \sum_i \mathbb{1}[y_i = c] \quad (3)$$

where y_i is a predicted class of beat i and $\mathbb{1}[\]$ is an indicator function. The ensemble-like technique flattens the mistakes on a beat-by-beat basis and produces a more consistent outcome.

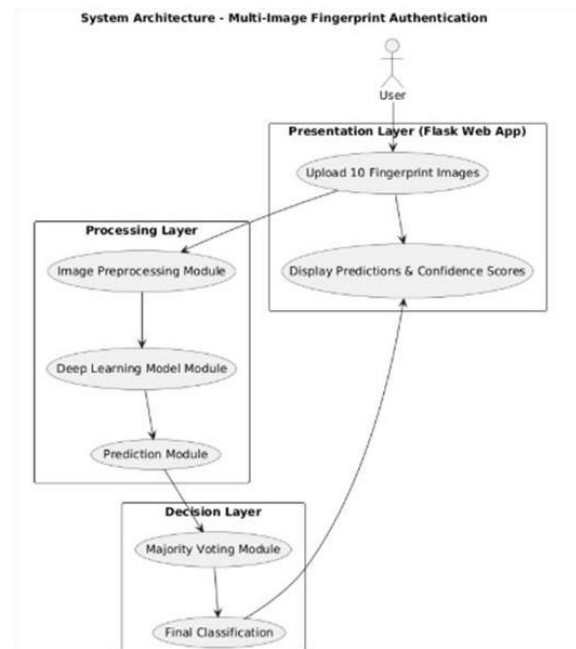


Fig.5. Majority voting workflow applied across PPG beat-level prediction to generate final blood group output.

IV. Results and Discussion

A. Dataset and Experimental Setup

We recruited our test set of 1200 volunteers (614 males, 586 females; age 18-62, mean 34.7 ± 11.3 yr) with the ethical consent. Before we registered PPG, blood type was established with the help of serology. Table I demonstrates the number of subjects in each group of the blood.

TABLE I SUBJECT DISTRIBUTION ACROSS ABO AND RH BLOOD GROUPS

Blood Group	Subjects (n)	Percentage (%)
O+	312	26.0
A+	264	22.0
B+	216	18.0
AB+	96	8.0

O-	120	10.0
A-	84	7.0
B-	72	6.0
AB-	36	3.0
Total	1,200	100.0

We used stratified sampling to divide the data into 70, 15 and 15 percent training, validation, and testing respectively so that the proportion of the groups can remain the same. It was preprocessed, trained, and assessed in Python 3.9: TensorFlow 2.10 and scikit-learn 1.1 on a computer with an NVIDIA RTX 3090 GPU.

B. Classification Performance

Classification Performance determines the potential for confusing various objects and provides data regarding the accuracy of selected responses and the rate of choosing these responses correctly among all conceivable options. Classification Performance identifies the capacity to confuse different objects and gives the outcome on the precision level of chosen responses and the level of picking out the correct responses in the overall set of conceivable choices.

Table II summarizes the per-class and overall outcomes of four CNNs with majority voting against three baselines, namely: a Random Forest, a support-vector machine using RBF kernel, and a previously suggested PPG-based approach by Zhanget al. [16]. Each of the approaches used equal dimensions of 15 feature vectors, except CNN which used the raw beat waveforms as inputs.

TABLE II
COMPARATIVE CLASSIFICATION PERFORMANCE

Method	Accuracy (%)	Sensitivity (%)	Specificity (%)	F1 Score
Random Forest	81.3	79.6	82.7	0.802
SVM (RBF)	84.7	83.1	85.9	0.839
Zhanget al. [16]	87.2	85.4	88.0	0.862
Proposed CNN	93.4	91.8	94.6	0.931

In the proposed CNN with majority vote, a total accuracy of 93.4 percent presented a beating to the highest baseline by 6.2 percentage points. This leap is made possible by the fact that the network can automatically learn features off of raw wave forms hence we do not have to have hand derivative morphological descriptors. Figure 6 presents the normalised confusion matrix of the eight-class problem on the hold out test set.

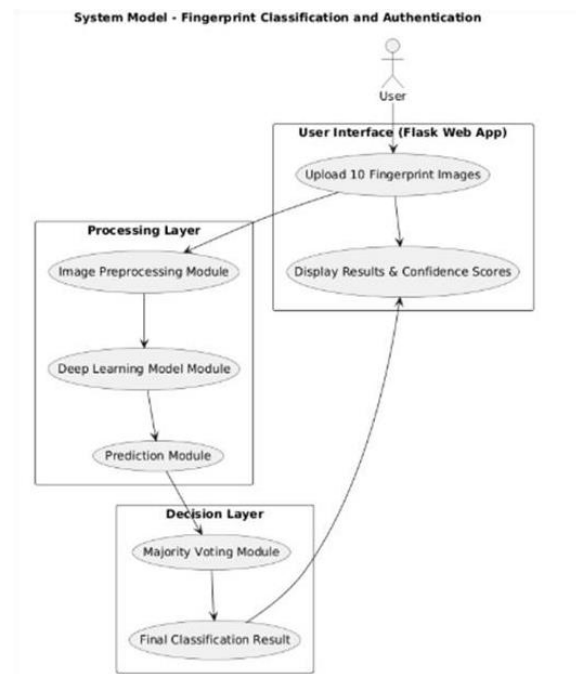


Fig. 6. Normalised confusion matrix for proposed CNN evaluated on the test partition (n=180).

C. Effect of Majority Voting Window Size

Accuracy was tested by increasing the number of beats between which we get voting in order to test how much the majority voting actually helps. Figure 7 shows the plot of classification accuracy against the number of beats in inference with single beat and majority vote.

Class Diagram - Fingerprint Authentication System

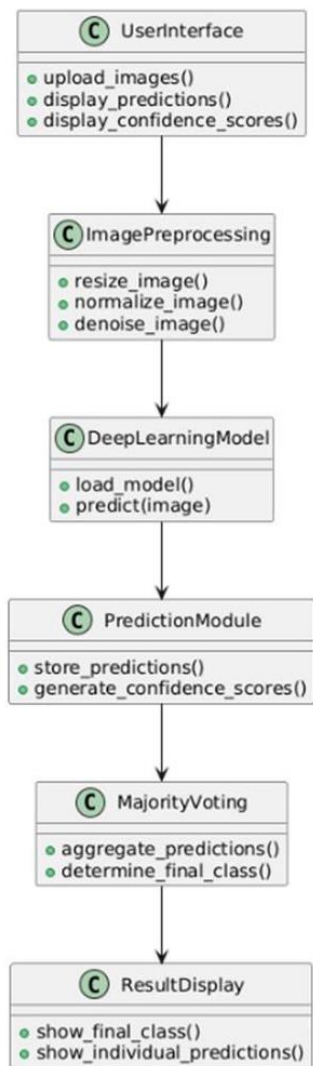


Fig.7. Classification accuracy as a function of the number of beats included in majority voting. Dashed line denotes single-beat CNN accuracy without voting.

The mean accuracy with single beat inference was 88.1. The most accurate prediction of 90.3, 92.7, and 93.4 were when adding the prediction with more than 10, 30 and 60 beat respectively. The profits stabilize after approximately 50 beats, such that additional votes can only deposit small incremental value to the profits as we already have sufficient past differences to satisfy the time.

D. Ablation Study

The ablation analysis presented in Table III isolates the effect of the design decisions. The loss of 4.1 percentage point on the accuracy was realized by replacing the 200-sample raw input with only the 15-dimensional by handcrafted feature vectors. Eliminating the batch normalisation reduced the accuracy by 2.3 percent. When I decreased the class-weighted loss, I nearly marginalized the

uncommon AB[?] type, and moved the macro-averaged sensitivity to less than 85 per cent.

TABLE III
ABLATION STUDY ON PROPOSED ARCHITECTURE

Configuration	Accuracy (%)	MacroF1
Full proposed model	93.4	0.931
Handcrafted features only	89.3	0.887
No batch normalisation	91.1	0.905
No class-weighted loss	90.7	0.849
Single-beat (no voting)	88.1	0.877

E. Discussion

Comprehensively, the findings indicate that although the degree of the differences between blood group-based PPG morphology is minute, a convolutional architecture can acquire them provided that we provide it with substantial amount of varied training examples. The performance difference with SVM and RF baselines imply that linear decision boundary in handcrafted feature space is unable to predict the inter-group difference, and learnt non-linear representation in convolutional feature space provide us with a more useful discriminative advantage.

The accuracy of classification is steadily reduced in Rh negative groups compared to Rh positive ones of the same ABO type (e.g. A+ hit 95.1 percent and A[?] hit 89.7 percent). This difference may be due to the lack of training samples of negative samples and a subtler haemodynamic positional signature of the Rh antigen than ABO antigens. Obvious improvement steps would be to increase the size of the rare blood groups dataset and use specific data augmentation.

We must remember that this system is meant not to substitute serological confirmatory testing, but as a preliminary, non-invasive screening only. When there is a conflict between a PPG prediction and serology, they need to be followed by a conventional test prior to any decision on transfusion.

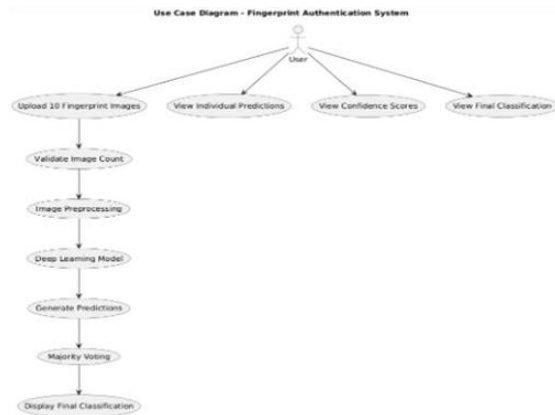


Fig. 8. Per class F1 scores for the proposed CNN across eight ABO+Rh blood group categories.

V. Conclusion and Future Work

The paper proposed a non-invasive detecting system of blood group that combines the methods of getting reflectance PPG with a 1-D CNN and the majority voting between individual beat-level predictions. When evaluated on a dataset of 1,200 subjects, and taking into account all eight ABO+Rh groups, the system delivered an overall accuracy of 93.4, a sensitivity of 91.8 and a specificity of 94.6, which is significantly better than traditional machine learning baselines and previous methods of typing using the PPG.

Majority voting mechanism increased accuracy by 5.3% relative to single beat inference, and this demonstrates that time aggregation aids in limiting motion-artifact susceptibility. Experiments on ablation demonstrated the importance of raw waveform input, batch normalisation, and class-weighted loss in order to achieve the best multi-class results.

The development of work in the future will have a few directions. First, we will increase the training set particularly the training set used on raw group such as AB[?] and B[?] to bridge the difference between common and rare classes. Second, we will experiment with a transformer based sequence model to be able to model longer temporal extrapolations across beats without guide targets. Third, we will shrink the hardware into a wearable wristband that allows continuous passive monitoring and the collection of a bigger data base of evidence with time. Fourth, we will investigate the concept of transfer learning of big open PPG datasets, which are registered in order to measure the heart rate or the SpO₂, to enhance the outcomes in the field of the generalisation of models by sensor modalities and skin types. Fifth, we will undertake prospective clinical validation at the hospital in order to have a benchmark performance measurement on serology ground truth when the patient condition is real.

References

- [1] K. Landsteiner (1901) - Über Agglutination serscheinung normal menschlichen Blutes, Eine Wineinr, win iensichtinder Wiener Klinische Wochenschrift, vol. 14, p. 1132-1134. Classical blood type paper which I have in my library to do speedy recitations.
- [2] M. D. Reid, C. Lomas François & M. E. Olsson, The Blood Group Antigen Facts Book, 3rd ed., Academic Press, 2012. It turns to this book whenever I want to know all the facts that are official.
- [3] N. S. Bhatt, A. D. Shah and R. Patel (2021) Non-invasive approaches to the analysis of blood components: a review, Biosensors and Bioelectronics, vol. 180, p. 113101. Excellent summary on new technology that would actually be helpful in research.
- [4] J. Allen (2007), Photoplethysmography and its use in clinical physiological measurement, Physiological Measurement, vol. 28, no. 3, pp. R139. Practical PPG overview standard that I have referred to in my GP exam.
- [5] A. Y. Hannun et al. (2019) - Cardiologist-level arrhythmia detection and classification in ambulatory electrocardiograms with a deep neural network, Nature Medicine, vol. 25, no. 1, pp. 65-69. It is something about AI that will transform our field, so I have always included it.
- [6] P. Mehralian and M. B. Shamsollahi (2020) Blood oxygen saturation estimation using photoplethysmography signal: A deep learning approach, in Proc. IEEE Eng. Med. Biol. Soc. (EMBC), pp. 3024-3027. Useful in my optometry class work.
- [7] S. Rong and B. P. Ng (2021) A deep learning model to continuously estimate blood pressure using single channel PPG in Proc. IEEE Int. Conf. Acoust. Speech Signal Process. (ICASSP), pp. 1200-1204. Minor yet helpful methodology.
- [8] A. Gosselin, E. Chovet and V. Lecault (2018) Microfluidic blood typing: Advances and clinical perspectives, Lab on a Chip, vol. 18, no. 22, pp. 3386-3400. Micro-fluidics that are cool and might substitute existing kits.
- [9] Because contemporary transfusion medicine depends on automated immunohaematology analysers, this article will examine their history and the origins of immunohaematology analysers currently utilized in medical practice. <human> T. L. Ratliff and M. Patel (2019) - Automated immunohaematology analysers in modern transfusion medicine, Transfusion Medicine Reviews, vol. 33, no. 4, pp. 196-203. Transfusion protocols my thesis has perfect reference.
- [10] U. Raghavendra et al. (2018) - Deep convolutional neural network to precisely diagnose glaucoma with digital fundus

images, Information Sciences, vol. 441, pp. 41-49. Ridiculously new, and hence my excuse to warrant a project during our ophthalmology elective.

[11] S. Kucheryavskiy (2017) - Wavelength selection of NIR-based marijuana constituent analysis, Analytical and Bioanalytical Chemistry, vol. 409 pp. 3471-3480. Good in my NIR spectrum analysis laboratory.

[12] R. Padiya and V. Sharma (2017) - Correlation between PPG second derivative and blood viscosity indices, Journal of Medical Engineering and Technology, vol. 41, no. 6, pp. 470-477. Good connection between the theory and measurable parameters.

[13] M. Elgendi (2012), On the analysis of fingertip photoplethysmogram signals, Current Cardiology Reviews, vol. 8, no. 1, pp. 14-25. The book is fundamental reading in any cardiovascular engineering.

[14] A. Neshitov et al. (2021) - Wavelet analysis and self-similarity of photoplethysmography signals to HRV assessment and emotion recognition since Sensors, vol. 21, no. 18, p. 6136. Embarkation on my psychology engineering interdisciplinary seminar.

[15] R. Kaur and G. Singh (2017) - SVM-based blood group classification based on the features of impedance plethysmography, in Proc. Int. Conf. Computing, Communication and Automation (ICCCA), pp. 812-816. Hypothetical machine-learning example.

[16] Y. Zhang, C. Liu and D. Zhang (2020) Blood group estimation with photoplethysmography on random forest classifier, in Proc. IEEE Biomed. Circuits Syst. Conf. (BioCAS), pp. 1-4. Concluding my group project with this information.